Factors affecting web-shear capacity of hollow-core slabs with filled cores

Scott A. Asperheim and Benjamin Z. Dymond

- Forty tests were performed on 20 prestressed concrete hollow-core slabs fabricated with either no core fill, cores filled with concrete or grout, or one void omitted during fabrication to investigate how core fill affects the web-shear capacity of hollow-core slabs.

- The test results were compared with predicted capacities calculated using the American Concrete Institute's *Building Code Requirements for Structural Concrete (ACI 318-14) and Commentary (ACI 318R-14)* and the European Committee for Standardization's *Precast Concrete Products—Hollow Core Slabs*, EN 1168.

- The results indicated that adequate composite action between the core-fill material and extruded slab was necessary to realize web-shear capacity gains, and the prestressing strand jacking stress, concrete compressive strength at transfer, transfer length, and moment demand can have a large effect on the web-shear capacity of a hollow-core slab.

PCI Journal (ISSN 0887-9672) V. 66, No. 4, July–August 2021.

PCI Journal is published bimonthly by the Precast/Prestressed Concrete Institute, 8770 W. Bryn Mawr Ave., Suite 1150, Chicago, IL 60631.

Precast, prestressed concrete extruded hollow-core slabs are cast with longitudinal voids along the length of the slab, which reduces both material quantities and member self-weight while maintaining the internal moment arm that results in high flexure capacities and the ability to span longer distances. However, because of the manufacturing process, shear reinforcement cannot be included when extruded hollow-core slabs are cast, which can result in limited shear capacities. To address this issue, extruded hollow-core manufacturers commonly fill one or more of the voids with concrete or grout at shear-critical areas; alternatively, they may reconfigure the extrusion machine to omit one or more of the voids completely as a means to increase the cross-sectional area that resists shear and therefore presumably increase the shear capacity of hollow-core slabs.[1]

Background

Manufacturers have been filling one or more voids of a hollow-core slab with concrete to increase the shear capacity since as early as the 1970s,[2] but limited research has been performed to validate the efficacy of filling cores or to quantify the capacity gained from the addition of core-fill concrete. In 1987, Anderson[3] proposed an equation to predict the increase in shear capacity from filling voids with concrete and attempted, but was unable, to verify this increase experimentally. In 2010, the Spancrete Manufacturers Association (SMA) released a research note[4] that proposed an equation to predict the increase in shear capacity gained by filling voids of Spancrete hollow-core slabs with grout. SMA verified the increased shear capacity by testing 40 in. (1020 mm) wide, 8 in. (200 mm) deep standard Spancrete slabs, but the test results used to verify an increased shear capacity from the use of core-fill grout were not available for review.

The European Committee for Standardization's (CEN's) *Precast Concrete Products—Hollow Core Slabs*, EN 1168,[5] provides shear capacity equations specifically for prestressed concrete hollow-core slabs, as well as an equation to calculate the capacity that is gained from the use of core-fill concrete. EN 1168 is largely based on previous research by Yang[6] and Pajari,[7,8] and it incorporates additional factors not considered when using the 2014 edition of the American Concrete Institute's *Building Code Requirements for Structural Concrete (ACI 318-14) and Commentary (ACI 318R-14)*.[9] These additional factors include moment demand, shear stress from the prestressing strands, and variation in cross-sectional geometries (for example, circular voids or noncircular voids).

While investigating the findings of Hawkins and Ghosh,[10] Palmer and Schultz[11] performed two tests on a 48 in. (1220 mm) wide, 16 in. (400 mm) deep hollow-core slab (one test on each end) where core-fill concrete was used in one of the four voids. Palmer and Schultz were unable to directly compare the experimentally determined shear capacities of the core-filled hollow-core slabs to empty slabs due to variation in testing variables (for example, concrete strength and the shear span–to–depth ratio a/d_p), but they concluded that the core fill "appear[ed] to provide a measurable increase" in the web-shear capacity.

McDermott and Dymond[12] investigated the effect that core-fill concrete had on the web-shear capacity of 48 in. (1220 mm) wide, 12 in. (300 mm) deep hollow-core slabs by testing each end of eight slabs (16 tests). Core-fill material was added immediately following extrusion or following detensioning to consider how core-fill timing affected web-shear capacity. In addition, several core-fill enhancement strategies were implemented and tested to investigate practical methods that may result in increased core-fill web-shear capacity. McDermott and Dymond concluded that the bond between the core-fill concrete and the extruded slab seemed to be the most important factor in obtaining additional web-shear capacity from the use of core-fill concrete.

Lee and colleagues[13] tested each end of three 47.2 in. (1200 mm) wide, 15.7 in. (400 mm) deep hollow-core slabs and each end of three 47.2 in. wide, 19.7 in. (500 mm) deep hollow-core slabs (12 tests). In these slabs, no core-fill concrete was present in one end and various types of core-fill concrete were placed in two of the four voids on the opposite end of each slab. The different types of core fill consisted of conventional cast-in-place concrete, steel-fiber-reinforced concrete, and core fill that included wire mesh. All core-fill material was added one week after the slabs were extruded, and all slabs were tested four weeks after the core-fill concrete was added. The investigators observed very brittle failures with no postcracking strength or ductility for all tests where no core-fill concrete was present; enhanced strength and ductility for core-filled slabs with depths of 15.7 in. after initial cracking occurred; and enhanced ductility but marginal strength gains for slabs with depths of 19.7 in. following initial cracking. Lee and colleagues concluded that a simple summation of the core-fill concrete shear capacity and the web-shear capacity of the extruded slab overestimated the total shear capacity of the member, and they proposed a method to predict the total shear capacity of hollow-core slabs that contained core-fill concrete.

Experimental program

The first objective of this experimental program was to quantify the amount of additional shear capacity that could potentially be gained by adding core-fill grout to one or more voids of a hollow-core slab, adding core-fill concrete to one or more voids of a hollow-core slab, or omitting a void when the extruded (dry-cast) hollow-core slabs were produced. The second objective of this program was to evaluate differences between ACI 318-14[9] and EN 1168[5] methodologies and predictions when calculating the shear capacity of hollow-core slabs with both circular and noncircular voids.

Hollow-core slab properties

The 20 extruded (dry-cast) hollow-core slabs tested as part of this program and described herein were provided by two different suppliers. Each hollow-core slab was tested twice, once at each end (sides A and B), to maximize the amount of data gathered. **Figure 1** presents the different supplier-specific cross sections that were tested as part of this research program. Cross sections with both noncircular voids (supplier A) and circular voids (supplier B) were tested to evaluate how variations in cross-sectional geometry may affect the shear capacity of hollow-core slabs as proposed by Yang,[6] Pajari,[7,8] and EN 1168.[5]

Supplier A provided eight heavy-duty 48 in. (1220 mm) wide, 12 in. (300 mm) deep hollow-core slabs that were 20 ft (6.1 m) long. The hollow-core slabs were cast with five noncircular voids and had thick webs. The nominal web thicknesses at the centroidal axis for exterior and interior webs were approximately 3 and 3.4 in. (75 and 86 mm), respectively. Four of the eight slabs provided by supplier A had core-fill concrete placed in two of the five voids; filling more than two of the voids was not considered as it was predicted that this would result in flexure-shear or flexural failures when testing was performed. Variations in the prestressing strand profiles and core-filling methods were also investigated for supplier A slabs and are discussed in more detail in the following sections.

Supplier B provided 12 standard 48 in. (1220 mm) wide, 12 in. (300 mm) deep hollow-core slabs that were 23 ft (7.0 m) long. The slabs were cast with four circular voids and had tapering webs. The nominal web thicknesses at the centroidal axis for exterior and interior webs were approximately 1.8 and 1.9 in. (46 and 48 mm), respectively. Within this set, supplier B modified its extrusion machine

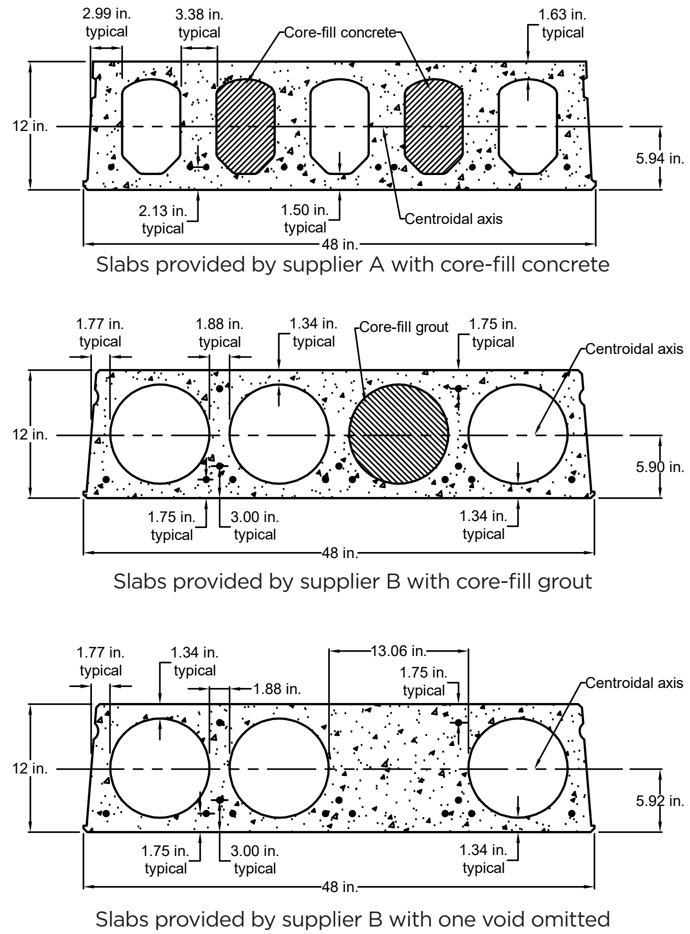

Figure 1. Cross-sectional geometries of hollow-core slabs. Note: 1 in. = 25.4 mm.

by removing one of the four void forms (**Fig. 2**) and cast four slabs with one of the four voids omitted. It was not possible to test slabs that had more than one of the four voids omitted due to the increased member weight that would be associated with the omission of additional voids. To allow for a direct comparison with slabs cast with a void omitted, supplier B also cast slabs that had core-fill grout placed in one of the four circular voids and slabs that did not omit voids and did not contain any core-fill grout (that is, slabs that had the typical cross section obtained when using the unmodified extrusion machine).

Table 1 presents a slab designation system for the different supplier-specific cross sections, prestressing strand patterns, and core-filling methods. Slab designations are presented in the format of S-#-#F, where S represents the supplier, # represents the strand type designation, and #F represents the number of cores that were filled and the type of core-fill material that was used. For example, A-1-NF is used to designate that the slab was provided by supplier A, was cast using strand pattern type 1, and no core-fill concrete was present.

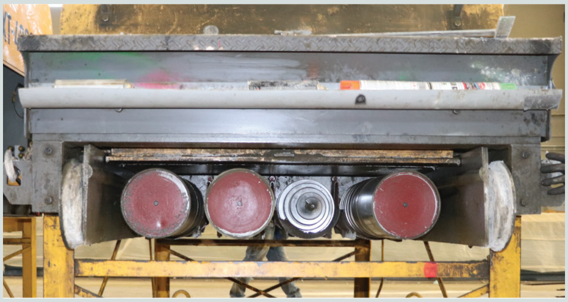

Figure 2. Extrusion machine that was used by supplier B to cast slabs with a void omitted (slab type B-3-1E). The silver auger is visible after removing a void form.

Prestressing strand properties

All hollow-core slabs were manufactured using seven-wire, 270 ksi (1860 MPa) low-relaxation prestressing strands. The

Table 1. Slab designation system for the tested hollow-core slabs based on the supplier, prestressing strand pattern type, and core-filling method

Supplier	Strand pattern number	Strand pattern description	Core fill designation	Number of cores filled and core-fill material type
Supplier A	1	Two 0.5 in. diameter strands and eight 0.6 in. diameter strands, all tensioned to $0.7f_{pu}$ and y_s of 2.125 in.	NF	No core fill
	2	Six 0.5 in. diameter strands and four 0.6 in. diameter strands, all tensioned to $0.7f_{pu}$ and y_s of 2.125 in.	2C	2 concrete-filled cores, a length of 48 in. on each end
			2R	2 roughened concrete-filled cores, a length of 48 in. on each end
Supplier B	3	Eight 0.5 in. diameter strands tensioned to $0.75f_{pu}$ and y_s of 1.75 in., three 0.5 in. diameter strands tensioned to $0.75f_{pu}$ and y_s of 3 in., and two 0.5 in. diameter strands tensioned to $0.5f_{pu}$ and y_s of 10.25 in.	NF	No core fill
			1E	1 extruded solid core over the entire length of the slab (that is, extrusion machine modified to omit one void)
			1G	1 grout-filled core, a length of 66 in. on each end

Note: Example designation system: A-1-NF designates that the slab was provided by supplier A, was cast using strand pattern type 1, and that no core-fill concrete was present. All strands were seven-wire, low-relaxation strands with an ultimate tensile strength. f_{pu} = 270 ksi; y_s = the centroid of the strand layer with respect to the slab bottom. 1 in. = 25.4 mm; 1 ksi = 6.895 MPa.

manufacturer's typical strand pattern that provided the maximum flexural capacity (Table 1) was selected for most slabs to help ensure that shear failure occurred during testing; however, two slabs provided by supplier A were cast with a strand profile that resulted in a slightly lower total prestressing force to investigate the findings of Truderung and associates,[14] who found that high total prestressing forces could result in reduced web-shear capacities when compared with identical slabs that were cast with lower total prestressing forces. In addition, the cross-sectional geometries tested by Truderung and associates were almost identical to the supplier B slabs that were tested as part of this program. The strand pattern for supplier B slabs had a jacking stress (ratio of jacking force F_j to cross-sectional area A_c) of approximately 1.20 ksi (8.27 MPa) at the neutral axis. This stress fell between the medium jacking stress of 1.00 ksi (6.89 MPa) and the high jacking stress of 1.48 ksi (10.20 MPa) investigated by Truderung's team, which provided an opportunity to examine their finding of reduced web-shear capacity with high total prestressing force.

Slab and core-fill manufacturing methods

Each hollow-core supplier used its typical core-filling method when manufacturing the test slabs to determine whether web-shear capacity gains from the addition of core-fill concrete or grout were being realized. Supplier A added core-fill concrete in the following manner:

1. Completely remove the top flange above the void area to be filled immediately following slab extrusion.

2. Form plugs using the top-flange material that was removed to contain the core-fill concrete on each end of the area to be filled.

3. Add a more workable concrete (obtained by adding water and a superplasticizer to the same no-slump concrete that was used to cast the slabs during the extrusion process) to the void area to be filled.

4. Finish the top flange by hand, cover the core-filled slab, and cure the slab on a heated casting bed.

5. Transfer the prestressing force to the continuous slab by uniformly detensioning all the strands at one end of the continuous slab. The individual slabs were cut to length from the continuous slab.

Supplier B added core-fill grout (which had 0.375 in. [9.53 mm] coarse aggregate) in the following manner:

1. Immediately following slab extrusion, remove approximately 12 in. (300 mm) long sections of the top flange, leaving sections of top the flange intact to prevent the narrow webs from collapsing.

2. Insert foam plugs into the voids at each end of the area to be filled to contain the grout.

3. Pump the core-fill grout mixture into the void area to be filled.

4. Finish the top surface by hand, cover the core-filled slab, and cure the slab on a heated casting bed.

5. Transfer the prestressing force to the continuous slab by individually flame cutting each strand at one end of the continuous slab. The individual slabs were cut to length from the continuous slab.

Supplier A also cast two slabs where the void walls were mechanically roughened prior to placing the core-fill concrete. The sidewalls of the voids were roughened using stiff bristles that were attached to two of the five void forms (**Fig. 3**). The bristles raked the sides of the voids as the extrusion machine traveled down the casting bed. After removing the top flange above the void area to be filled, the bottom of the void was also hand raked using a stiff-bristle brush formed to fit the tapering portion of the webs of the void. After roughening the slab concrete, supplier A proceeded with its typical core-filling procedure.

Figure 3. The bottom of an extrusion machine used by supplier A to roughen the sidewalls of the voids. Two void forms were fitted with stiff bristle attachments.

Hardened material properties

Hardened concrete and grout properties were determined using 4 in. (100 mm) diameter, 8 in. (200 mm) tall cylinders that were cast when the test slabs were extruded and when the core-fill concrete or grout was placed in the void or voids, if present. Three cylinders of extruded concrete and three cylinders of core-fill material, if present, were typically cast for each end of each slab to be tested. The compressive strengths of the slab cylinders f_c' and core-fill cylinders f_{cf}' were determined in accordance with ASTM C39 *Standard Test Method for Compressive Strength of Cylindrical Concrete Specimens*[15] on the date that the slab shear test was performed. Both hollow-core suppliers cast cylinders of extruded hollow-core slab concrete and provided the concrete compressive strength at transfer $f_{c,transfer}'$ when the prestressing force was transferred to the continuous slab. Hardened material properties for each of the slabs manufactured by supplier A and supplier B are shown in **Tables 2** and **3**.

Test setup

During each test on a slab, the load was applied 30 in. (760 mm) from the centerline of the nearest roller support and 162 in. (4.11 m) from the centerline of the far, pinned support. The supports were constructed using neoprene bearing pads, steel plates, steel cylinders, and additional steel channels where necessary. The testing geometry was selected to achieve a shear span *a*–to–depth d_p ratio of 3.0 to avoid arching action. This value corresponded with a shear span *a*–to–height *h* ratio of 2.5 considering the entire section depth. This was selected because the hollow-core slabs were not expected to have flexural cracking before web-shear failure. Load was distributed across the width of the slab using a grout pad and neoprene bearing pad. The test setup is shown in **Fig. 4**.

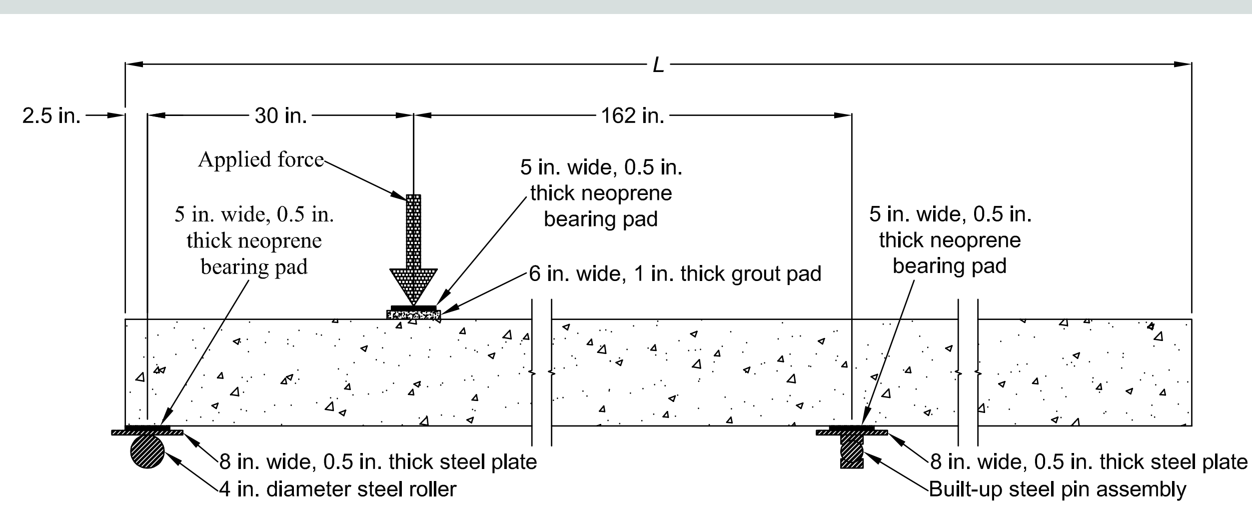

Figure 4. Elevation view of the test setup. Note: *L* = length of hollow-core section = 240 and 276 in. for slabs provided by suppliers A and B, respectively. 1 in. = 25.4 mm.

Table 2. Experimental results for all slabs provided by supplier A

Slab type	Test number	Loading method	Failure mode	Test age, days	$f'_{c,transfer}$, psi	f'_c, psi	f'_{cf}, psi	Peak applied load, kip
A-1-NF	1A	LF	WS	72	4510	12,540*	n/a	99.0
	1B	LF	WS	73	4510	12,540*	n/a	84.0
	2A	LF	WS	77	4510	12,540*	n/a	91.8
	2B	LF	WS/FS	80	4510	12,540*	n/a	89.2
Average				76	4510	12,540*	n/a	91.0
A-1-NF	17A	LF	WS	42	6640	12,050	n/a	117.9
	17B	LF	WS	43	6640	11,950	n/a	116.0
A-2-NF	16A	LF	WS	40	5880	12,050	n/a	122.8
	16B	LF	WS	41	5880	12,120	n/a	120.5
Average				42	6260	12,043	n/a	119.3
A-1-2C	3A	LF	WS	22	3600	9430	7180	83.9
	3B	LF	WS/FS	23	3600	n.d.†	n.d.†	101.5
	4A	LF	WS	28	4340	10,880	7110	83.4
	4B	LF	WS	29	4340	11,010	7160	102.6
Average				26	3970	10,440	7150	92.8
A-1-2R	5A	LF	WS	23	4130	11,850	6920	92.4
	5B	LF	WS	25	4130	11,230	7160	113.5
A-2-2R	6A	LF	WS	30	4130	11,210	7020	98.3
	6B	LF	WS	30	4130	11,210	7020	111.2
Average				27	4130	11,375	7030	103.9

Note: See Table 1 for slab type descriptions. f'_c = nominal compressive strength of hollow-core slab concrete when tested; f'_{cf} = average compressive strength of core-fill material on slab test day; $f'_{c,transfer}$ = concrete compressive strength at prestressing transfer; FS = flexure shear; LF = load frame (rather than spreader beam); n/a = not applicable; n.d. = no data; WS = web shear. 1 psi = 6.895 kPa; 1 kip = 4.448 kN.

*Average compressive strength determined using three cylinders tested over a range of six days.

†Cylinder testing machine was inoperable when test 3B was performed.

Load application

A 110 kip (489 kN) hydraulic actuator was used to test the hollow-core slabs in this program. Web-shear capacity predictions showed that this magnitude of applied load would be insufficient to obtain web-shear failures in the heavy-duty slabs with large web widths provided by supplier A. To address this, a structural steel frame was fabricated to act as a lever mechanism and allow for the load applied to the hollow-core slabs to be increased without exceeding the 110 kip rating of the hydraulic actuator. The structural steel frame had a 2-to-1 ratio between the fulcrum points so that the compressive load applied to hollow-core slabs was approximately double the tensile force recorded by the internal load cell on the hydraulic actuator. The frame assembly was independently calibrated using a portable load cell to verify the multiplication factor, which showed that the load applied to a specimen was 1.97 times greater than the tension applied by the actuator, with a coefficient of determination equal to 1.00 based on 32 data pairs. Using this structural steel frame, a wide flange steel cross member applied load to the top of the hollow-core slabs. Alternatively, a stiffened steel spreader beam was directly attached to the hydraulic actuator (without the structural steel frame) and used for four of the eight tests performed on slab type B-3-1E and four of the eight tests performed on slab type B-3-NF as a secondary means of verifying the load applied by the structural steel frame. **Figure 5** shows both the structural steel frame and the stiffened spreader beam. Load was typically applied to the slabs at a displacement-controlled rate of 0.0003 in./sec (0.0076 mm/sec) for all tests.

This magnitude of applied load is representative of the line and point loads often encountered in a podium structure. The procedure for distributing point and line loads used in

Table 3. Experimental results for all slabs provided by supplier B

Slab type	Test number	Loading method	Failure mode	Test age, days	$f'_{c,transfer}$, psi	f'_c, psi	f'_{cf}, psi	Peak applied load, kip
B-3-1E	7A	LF	WS	28	3630	9630	n/a	64.3
	7B	LF	WS	29	3630	10,370	n/a	58.5
	8A	LF	WS	29	3850	9640	n/a	59.0
	8B	LF	WS/FS/BF	32	3850	9310	n/a	47.6
	9A	SB	WS	29	3670	10,270	n/a	56.7
	9B	SB	WS	35	3670	10,100	n/a	49.6
	10A	SB	FS	41	4050	10,460	n/a	57.6
	10B	SB	WS	44	4050	10,900	n/a	57.2
Average				33	3800	10,090	n/a	56.3
B-3-1G	11A	SB	WS	48	4050	9960	8520	62.3
	11B	SB	WS	49	4050	10,030	8720	61.7
	12A	SB	WS	50	4310	11,800	9750	47.7
	12B	SB	WS	51	4310	11,620	9530	57.0
	13A	SB	WS	61	4310	11,030	9330	55.5
	13B	SB	WS	63	4310	10,970	9370	59.8
	14A	SB	WS	69	4090	11,520	8750	63.5
	14B	SB	WS	70	4090	11,630	9070	57.8
Average*				59	4170	10,970	9040	59.7
B-3-NF	15A	SB	WS	73	4090	11,610	n/a	60.1
	15B	SB	WS	74	4090	11,190	n/a	60.6
	18A	LF	WS	87	3850	11,250	n/a	59.5
	18B	LF	WS	88	3850	11,420	n/a	66.8
	19A	LF	WS	85	3920	10,440	n/a	54.2
	19B	LF	WS	86	3920	10,350	n/a	49.3
	20A	SB	WS	91	3850	11,030	n/a	55.0
	20B	SB	WS	92	3850	11,390	n/a	64.8
Average				85	3930	11,090	n/a	58.8

Note: See Table 1 for slab type descriptions. BF = bond failure; f'_c = nominal compressive strength of hollow-core slab concrete when tested; f'_{cf} = average compressive strength of core-fill material on slab test day; $f'_{c,transfer}$ = concrete compressive strength at prestressing transfer; FS = flexure shear; LF = load frame; n/a = not applicable; SB = spreader beam; WS = web shear. 1 psi = 6.895 kPa; 1 kip = 4.448 kN.

*Test 12A was excluded from the averages because premature failure occurred during the test near the applied load due to nonuniform bearing at the near support.

practice[1] is not intended to represent the actual load path through the hollow-core slab; rather, it is a model based on testing to provide values for design. This procedure is generally considered conservative. The method defines an effective resisting width equal to half of the span length at midspan, but the effective width is only 4.0 ft (1.2 m) at the support. This means that flexural resistance is obtained from multiple hollow-core slabs, but shear resistance is only obtained from a single hollow-core slab. This methodology can yield a high shear demand at the support and may result in hollow-core sections with very wide webs and filled cores as tested herein.

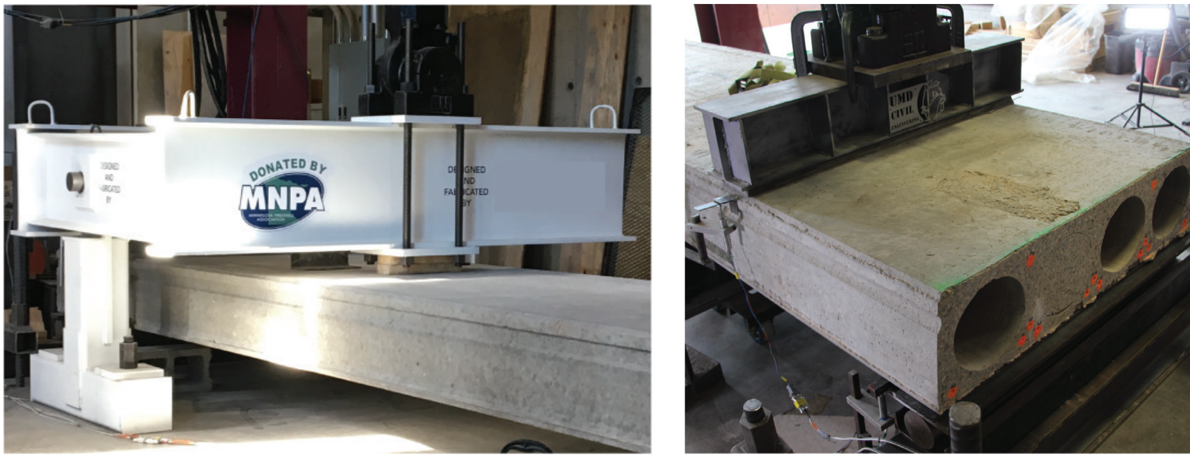

Structural steel frame

Stiffened spreader beam

Figure 5. The structural steel frame straddling a hollow-core slab and a stiffened spreader beam attached to a hydraulic actuator used to apply load to a hollow-core slab with one grout-filled core.

Instrumentation and documentation

An internal linear variable displacement transducer (LVDT) and 100 kip (445 kN) capacity load cell were used to measure actuator displacement and applied force, respectively. In addition, three pairs of external LVDTs were used to measure slab displacement on each side of the slab at the near support, the load point, and the far support. Data from these LVDTs were used to evaluate the extent of any torsional stresses due to nonuniform bearing or loading that may have been induced during testing, which would be indicated by differential displacement between the paired LVDTs and between the different LVDT sets. Pre- and posttest strand slip measurements were also recorded for all strands using a digital tire-tread-depth gauge. The second end of each slab (side B) was dismantled after diagonal web-shear failure occurred to expose the failure plane, and a three-dimensional (3-D) model of the crack face was generated using an Artec 3-D scanner. The 3-D models were used to measure the crack angles of the failure planes and allowed for a comparison of test data even after broken slabs were discarded.

Shear prediction methods

ACI 318-14

The web-shear capacity V_{cw} of prestressed concrete members is predicted by ACI 318-14[9] Eq. (22.5.8.3.2). Eq. (1) is ACI 318-14[9] Eq. (22.5.8.3.2) converted for SI units.

$$V_{cw} = \left(3.5\sqrt{f_c'} + 0.3 f_{pc}\right) b_w d_p + V_p \qquad \text{(ACI 318-14 22.5.8.3.2)}$$

$$V_{cw} = \left(0.29\sqrt{f_c'} + 0.3 f_{pc}\right) b_w d_p + V_p \tag{1}$$

where

f_{pc} = compressive stress in concrete, after allowance for all prestress losses, at centroid of cross section resisting externally applied loads

b_w = width of web(s)

V_p = vertical component of effective prestressing force at section

All prestressed concrete hollow-core slabs tested as part of this program had horizontal prestressing strand profiles and, accordingly, V_p was equal to zero for all web-shear capacity predictions. The compressive stress in the concrete f_{pc} is a function of the transfer length of prestressed reinforcement l_{tr}, which was assumed to be equal to $50d_b$ (where d_b is the nominal strand diameter of the prestressing strand) in accordance with section 22.5.9.1 of ACI 318-14. Prestress losses were calculated using the simplified method provided in ACI's *Guide to Estimating Prestress Loss*, ACI 423.10R.[16]

It was assumed that core-fill material acted as nonprestressed concrete when calculating the additional shear capacity that was gained due to the presence of fill material for ACI 318-14 predictions. The shear capacity of nonprestressed concrete V_c is predicted using ACI 318-14 Eq. (22.5.5.1). Eq. (2) is ACI 318-14 Eq. (22.5.5.1) converted for SI units.

$$V_c = 2\sqrt{f_c'} b_w d \qquad \text{(ACI 318-14 22.5.5.1)}$$

$$V_c = 0.17\sqrt{f_c'} b_w d \tag{2}$$

where

d = distance from extreme compression fiber to centroid of longitudinal tension reinforcement

When predicting the combined shear capacity of the extruded hollow-core slab and core-fill material, the total area of the core-fill material proposed by Anderson[3] was used. Accordingly, all ACI 318-14 shear capacity predictions were calculated using Eq. (3). Eq. (4) is Eq. (3) converted for SI units.

$$V_{cw} = \left(3.5\sqrt{f'_c} + 0.3f_{pc}\right)b_w d_p + 2\sqrt{f'_{cf}}A_f n_f \tag{3}$$

$$V_{cw} = \left(0.29\sqrt{f'_c} + 0.3f_{pc}\right)b_w d_p + 0.17\sqrt{f'_{cf}}A_f n_f \tag{4}$$

where

A_f = cross-sectional area of filled core

n_f = number of filled cores

For test slabs where no core-fill material was present, the number of filled cores n_f was equal to zero and the predicted web-shear capacity was equivalent to that calculated using ACI 318-14[9] Eq. (22.5.8.3.2).

EN 1168

The general method of EN 1168[5] was also used to predict the shear capacity of hollow-core slabs tested as part of this program. The general method of predicting the shear capacity of the hollow-core slabs is presented as Eq. (5).

$$V_{Rdc} = \frac{I \times b_w(y)}{S_c(y)}\left(\sqrt{\left(f_{ct}\right)^2 + \sigma_{cp}(y) \times f_{ct}} - \tau_{cp}(y)\right) \tag{5}$$

where

$$\sigma_{cp}(y) = \sum_{t=1}^{n}\left\{\left[\frac{1}{A} + \frac{\left(Y_c - y\right)\left(Y_c - Y_{Pt}\right)}{I}\right] \times P_t\left(l_x\right)\right\} - \frac{M_{Ed}}{I} \times \left(Y_c - y\right) \tag{6}$$

and

$$\tau_{cp}(y) = \frac{1}{b_w(y)} \times \sum_{t=1}^{n}\left\{\left[\frac{A_c(y)}{A} - \frac{S_c(y) \times \left(Y_c - Y_{Pt}\right)}{I} + Cp_t(y)\right] \times \frac{dP_t\left(l_x\right)}{dx}\right\} \tag{7}$$

where

V_{Rdc} = shear resistance in regions uncracked by bending for prestressed concrete hollow-core slabs

I = second moment of area of the cross section

$b_w(y)$ = web width at the height y

y = height of critical point on the line of failure

$S_c(y)$ = first moment of the area above height y and about the centroidal axis

f_{ct} = actual tensile strength of concrete

$\sigma_{cp}(y)$ = full concrete compressive stress at height y and distance l_x

$\tau_{cp}(y)$ = concrete shear stress due to transmission of prestress at height y and distance l_x

l_x = distance of section considered from the starting point of the transmission length

A = fictive cross-section surface

Y_c = height of the centroidal axis

Y_{Pt} = height of the position of considered tendon layer

$P_t(l_x)$ = prestressing force in the considered tendon layer at a distance l_x

M_{Ed} = bending moment due to the vertical load

$A_c(y)$ = area above height y

$C_{pt}(y)$ = factor taking into account the position of the considered tendon layer

$\frac{dP_t\left(l_x\right)}{dx}$ = gradient of the prestressing force in the considered tendon layer at a distance l_x

The variable $\sigma_{cp}(y)$ represents the axial precompression of the concrete due to the prestressing strands, less the tensile stress due to the applied moment, at the height of the assumed failure location (and assuming the height of the assumed failure location is below the neutral axis). The tensile stress due to the applied moment M_{Ed} contributes to a loss of shear capacity because it is subtracted at the end of Eq. (6) and therefore subtracted from shear resistance in regions uncracked by bending for prestressed concrete hollow-core slabs V_{Rdc}. The variable $\tau_{cp}(y)$ represents the shear stresses due to the prestressing strands at the height of the assumed failure location and exists only within the transmission (transfer) length. This variable contributes to a loss of shear capacity because it is subtracted from shear resistance in regions uncracked by bending for prestressed concrete hollow-core slabs V_{Rdc} in Eq. (5). The general method of EN 1168 requires iterative calculations along a line of failure, which extends 35 degrees from the inner face of the near support (but not within a horizontal distance of one-half the member height h from the inner face of the support). The minimum value of the shear capacity found along this line is used for design. The assumption of a 35-degree crack angle was proposed by Yang[6] and based on finite element analysis. Eq. (5) was used to calculate the capacity for all slabs in this research program, even those with circular voids, which have a minimum web width at the centroidal axis and may fail along a shear plane other than 35 degrees.

In Eq. (5), f_{ct} is a function of the concrete compressive strength and is approximately equivalent to a diagonal tension strength of concrete f_t' of $3.5\sqrt{f_c'}$ psi, which is the ACI diagonal tension strength of concrete.[17,18] For design purposes, f_{ct} is designated as f_{ctd} and calculated as 70% of the mean value of the 28-day axial tensile strength of concrete using Eq. (3.16) from *Eurocode 2: Design of Concrete Structures—Part 1-1: General Rules and Rules for Buildings*, EN 1992-1-1.[19] However, for validation testing of hollow-core slabs, annex J.5 of EN 1168 requires that the actual tensile strength of concrete f_{ct} be calculated as 80% of the axial tensile strength of concrete on the day that the hollow-core slab test is performed. The actual tensile strength of concrete f_{ct} requirements for validation testing were used in this research program.

Transmission lengths used in EN 1168 capacity predictions were calculated in accordance with section 8.10.2.2 (2) of EN 1992-1-1; however, EN 1992-1-1 section 8.10.2.2 (3) requires that the transmission length be taken as 120% of the basic value of transmission length for shear design, which results in more-conservative capacity predictions. To analyze laboratory results in this research program, all capacity predictions were calculated using the basic value of the transmission length l_{pt}, and not $1.2 \times l_{pt}$. Time-dependent prestress losses were calculated in accordance with EN 1992-1-1.

Appendix F.3 of EN 1168 provides an equation to calculate the total shear tension capacity of a hollow-core slab with a number of filled cores V_{Rdt}, shown here as Eq. (8).

$$V_{Rdt} = V_{Rdc} + \frac{2}{3} \times n_f \times b_c \times d \times f_{ctd,f} \tag{8}$$

where

b_c = width of the cores

$f_{ctd,f}$ = design tensile strength of core-fill material

EN 1168 Fig. F.1, which shows core-fill concrete in hollow-core slabs with circular voids, implies that b_c should be taken as the maximum width of the core. This assumption was made for calculations performed as part of this program. It is not clear whether the ⅔ constant factor in Eq. (8) represents a shape factor that reduces the rectangular area obtained from the width of the cores b_c multiplied by the distance from the extreme compression fiber to the centroid of the longitudinal tension reinforcement d to account for the nonrectangular core fill or whether it is a reduction factor that accounts for the potential of noncomposite action between the core-fill material and the extruded slab.

Experimental results and comparisons with predicted web-shear capacity

Of the 40 tests performed, 36 web-shear failures occurred, two tests (tests 2B and 3B) resulted in a combined web-shear and flexure-shear failure, one test (test 8B) resulted in combined web-shear and flexure-shear cracking followed by strand slip when loading was continued, and one test (test 10A) resulted in a flexure-shear failure. The experimental results for all tests of supplier A and supplier B slabs are presented in Tables 2 and 3.

Slab displacement during testing

Displacement readings between the paired LVDTs at the near support, load point, and far support should be equal for a test where a symmetric slab is uniformly supported and loaded. Differences in displacement between one side of a test slab compared with the other (that is, differential displacement readings between the paired LVDTs) could indicate unintended torsional stresses or stress concentrations. **Table 4** presents the differential displacement recorded between the three LVDT pairs, along with the method of loading (load frame assembly or stiffened spreader beam) and peak applied load at failure for each test in this program. Various methods—such as the use of a grout pad or neoprene pad, shimming of the load frame, and shimming at the supports—were used to eliminate as much differential displacement between LVDT pairs as possible during testing.

Slabs with an extruded solid core

Slabs cast with an extruded solid core (that is, with one of the voids omitted), denoted as slab type B-3-1E, performed poorly compared with both of the evaluated prediction methods. On average, slab type B-3-1E failed at approximately 59% and 70% of the capacities predicted using ACI 318-14[9] and the general method of EN 1168,[5] respectively. (This paper does not provide a comparison of the experimental results to predicted values for slab type B-3-1E because of the slab type's poor performance, but the data can be found in Asperheim.[20]) A lack of symmetry may have contributed to the poor performance where the poorly compacted solid section attracted greater load than the other internal webs; shear failure in hollow-core slabs with different web widths is governed by the thinnest web width. Furthermore, it was concluded that the extruded concrete was not sufficiently compacted due to the void form being removed, and that resulted in a poor bond between the prestressing strands and extruded slab. This conclusion was supported by two findings: strand slip values up to 0.3 in. (7.6 mm) were recorded for prestressing strands near the omitted void, and low compressive and splitting tensile strength values were obtained from concrete cylinders that were removed from the extruded solid core section of slab 10 using a coring rig. The data supporting these findings can be found in Asperheim.[20] **Figure 6** presents pre- and posttest strand slip measurements for all tests.

ACI 318-14

Table 5 presents ACI 318-14[9] predicted failure locations, corresponding unfactored shear demand from self-weight and applied load V_{sw+app}, predicted slab and core-fill shear capacity

Table 4. Peak applied load and difference in displacement readings for paired linear variable displacement transducers located on each side of the slab at the near support, the load point, and at the far suppor

Slab type	Test number	Loading method	Peak applied load, kip	LVDT pair location and difference between the pair*		
				Near support, in.	Load point, in.	Far support, in.
A-1-NF	1A	LF	99.0	0.08	0.05	0.01
	1B	LF	84.0	0.09	0.06	0.04
	2A	LF	91.8	0.10	0.05	0.03
	2B	LF	89.2	0.10	0.06	0.05
	17A	LF	117.9	n/a	n/a	n/a
	17B	LF	116.0	0.01	0.02	0.00
A-1-2C	3A	LF	83.9	0.09	0.06	0.03
	3B	LF	101.5	0.07	0.04	0.02
	4A	LF	83.4	0.12	0.11	0.06
	4B	LF	102.6	0.12	0.11	0.06
A-1-2R	5A	LF	92.4	0.04	0.06	0.04
	5B	LF	113.5	0.02	0.02	0.02
A-2-NF	16A	LF	122.8	–0.01	–0.01	–0.01
	16B	LF	120.5	0.02	0.01	–0.01
A-2-2R	6A	LF	98.3	0.01	0.02	0.03
	6B	LF	111.2	–0.02	–0.01	0.00
B-4-1E	7A	LF	64.3	0.06	0.05	0.02
	7B	LF	58.5	0.08	0.08	0.05
	8A	LF	59.0	0.07	0.06	0.04
	8B	LF	47.6	0.04	0.02	0.01
	9A	SB	56.7	0.07	0.07	-0.03
	9B	SB	49.6	0.06	0.14	-0.14
	10A	SB	57.6	0.08	0.07	-0.03
	10B	SB	57.2	0.05	0.07	-0.03
B-4-1G	11A	SB	62.3	0.08	0.08	0.03
	11B	SB	61.7	0.12	0.07	-0.06
	12A	SB	47.7	0.05	0.16	0.00
	12B	SB	57.0	0.09	0.06	-0.05
	13A	SB	55.5	0.00	0.09	0.05
	13B	SB	59.8	0.01	–0.08	–0.06
	14A	SB	63.5	0.01	–0.03	–0.02
	14B	SB	57.8	0.00	–0.09	–0.07
B-4-NF	15A	SB	60.1	0.01	0.05	0.03
	15B	SB	60.6	0.00	–0.01	–0.01
	18A	LF	59.5	–0.01	0.00	–0.01
	18B	LF	66.8	–0.01	–0.01	–0.01
	19A	LF	54.2	–0.01	–0.01	–0.02
	19B	LF	49.3	0.03	0.03	0.02
	20A	SB	55.0	–0.07	–0.11	–0.06
	20B	SB	64.8	–0.04	–0.03	–0.02

Note: See Table 1 for slab type descriptions. LF = load frame; LVDT = linear variable displacement transducer; n/a = not available (due to LVDT failure early in the test); SB = spreader beam. 1 in. = 25.4 mm; 1 kip = 4.448 kN.

*Negative values indicate larger displacement in the south LVDT.

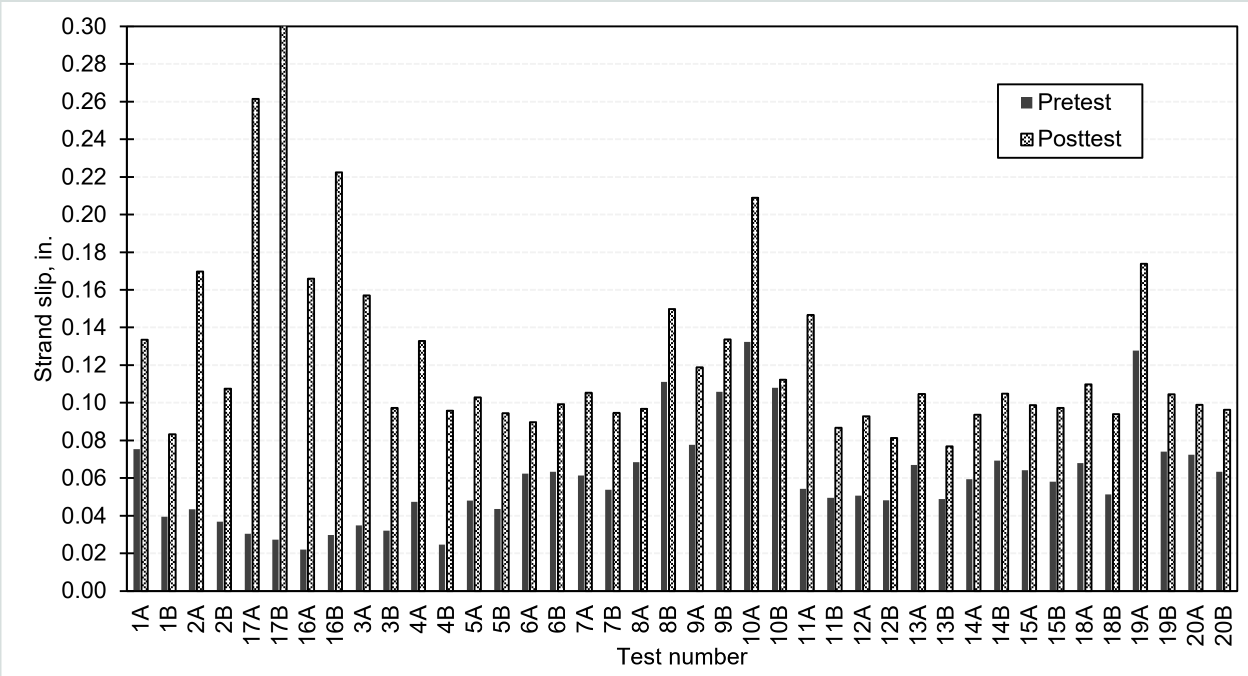

Figure 6. Average of pre- and posttest strand slip measurements for all tests. Note: 1 in. = 25.4 mm.

$V_{n,slab}$ plus unfactored nominal shear capacity of core-fill concrete or grout $V_{n,fill}$, and ratios of shear demand–to–capacity for all slabs (excluding slab type B-3-1E). In addition, the table presents the ratio of the moment demand from self-weight and applied load to the unfactored ACI 318-14 predicted moment capacity to show the contrast in loading demands between slabs provided by suppliers A and B.

Results in Table 5 show that average failures occurred at shear demands that were lower than the slab shear capacities predicted using ACI 318-14 for nine of the 16 tests performed on supplier A slabs. Slabs that had lower values of concrete compressive strength at transfer (Table 2) and no core-fill concrete (tests 1A, 1B, 2A, and 2B) failed in shear at an average of 83% (±6%) of capacity $V_{n,slab}$. Slabs with lower values of concrete compressive strength at transfer and core-fill concrete placed in unroughened voids (tests 3A, 3B, 4A, and 4B) failed in shear at an average of 93% (±11%) of capacity $V_{n,slab}$. Slabs with lower values of concrete compressive strength at transfer and core-fill concrete placed in roughened voids (tests 5A, 5B, 6A, and 6B) failed in shear at an average of 99% (±11%) of capacity $V_{n,slab}$. Slabs with higher values of concrete compressive strength at transfer and no core-fill concrete (tests 17A, 17B, 16A, and 16B) failed in shear at an average of 111% (±2%) of capacity $V_{n,slab}$. The larger variation in the ratio of shear demand V_{sw+app} to capacity $V_{n,slab}$ for slabs with core-fill concrete present was attributed to the fill material providing additional shear capacity for some, but not all, of the slabs that were tested. Failures occurring below the ACI 318-14 predicted shear capacity could be attributed to the large moment demand that was present when failures occurred. Alternatively, low failure loads could be due to unintended eccentricities generated from nonuniform bearing at the supports, nonuniformly distributed demand at the load point, or core-fill concrete that did not act uniformly composite in all of the filled voids. Testing an individual hollow-core slab with a single point load near the end of the span (which also generates high moment demand) likely does not accurately reflect the real-life load demand applied to a hollow-core slab floor system, where multiple hollow-core slabs placed side-by-side with grouted shear keys likely distribute moment demand and loading eccentricities.

Results in Table 5 also show that average failures occurred at shear demands that were higher than the slab shear capacities predicted using ACI 318-14 for all but one of the tests performed on supplier B slabs (excluding slab type B-3-1E). Supplier B slabs with core-fill grout in one void (slab type B-3-1G) failed in shear at an average of 113% (±9%) of capacity $V_{n,slab}$, and supplier B slabs with no core-fill grout (slab type B-3-NF) failed in shear at an average of 111% (±14%) of capacity $V_{n,slab}$. The concrete compressive strength at transfer (Table 3) was approximately equal for all supplier B slabs.

EN 1168

Table 6 presents the failure location predicted using the general method of EN 1168[5] (with the horizontal distance from the slab end to the predicted failure location x_{crit} and height of critical point on the line of failure y) and a comparison of the experimentally determined shear demand to the predicted shear capacity at this location. Results in Table 6 show that

Table 5. Comparison of ACI 318-14 predictions to experimental test results

Slab type	Test number	x_{crit},* in.	b_w, in.	d_p, in.	M_{sw+app}/M_n	V_{sw+app}, kip	$V_{n,slab}$, kip	$V_{sw+app}/V_{n,slab}$	$V_{n,fill}$, kip	$V_{sw+app}/(V_{n,slab} + V_{n,fill})$
A-1-NF	1A	11.00	19.49	9.88	0.90	86.04	95.10	0.90	n/a	n/a
	1B				0.77	73.63	95.10	0.77	n/a	n/a
	2A				0.83	79.94	95.10	0.84	n/a	n/a
	2B				0.81	77.74	95.10	0.82	n/a	n/a
Average		11.00	19.49	9.88	0.83	79.34	95.10	0.83	n/a	n/a
A-1-NF	17A	11.00	19.49	9.88	1.07	101.99	93.59	1.09	n/a	n/a
	17B				1.05	100.35	93.29	1.08	n/a	n/a
A-2-NF	16A				1.26	106.12	93.31	1.14	n/a	n/a
	16B				1.24	104.19	93.52	1.11	n/a	n/a
Average		11.00	19.49	9.88	1.16	103.16	93.43	1.11	n/a	n/a
A-1-2C	3A	11.00	19.49	9.88	0.78	73.28	84.82	0.86	14.80	0.74
	3B				0.94	88.17	84.82	1.04	14.80	0.89
	4A				0.77	72.83	89.82	0.81	14.73	0.70
	4B				0.94	89.09	90.24	0.99	14.78	0.85
Average		11.00	19.49	9.88	0.86	80.84	87.43	0.93	14.78	0.80
A-1-2R	5A	11.00	19.49	9.88	0.84	80.49	92.96	0.87	14.53	0.75
	5B				1.03	98.28	89.98	1.09	14.78	0.93
A-2-2R	6A				1.02	85.48	90.63	0.94	14.63	0.81
	6B				1.15	96.35	90.63	1.06	14.63	0.92
Average		11.00	19.49	9.88	1.01	90.15	91.05	0.99	14.64	0.85
B-3-1G	11A	11.00	9.13	9.91†	0.56	54.33	44.46	1.22	12.57	0.95
	11B				0.55	53.83	44.57	1.21	12.72	0.94
	12A				0.43	42.01	47.22	0.89	12.40	0.70
	12B				0.51	49.87	46.96	1.06	13.30	0.83
	13A				0.50	48.61	46.09	1.05	13.16	0.82
	13B				0.53	52.21	46.01	1.13	13.19	0.88
	14A				0.56	55.31	46.81	1.18	12.74	0.93
	14B				0.56	54.33	44.46	1.08	12.97	0.84
Average‡		11.00	9.13	9.91	0.54	52.64	45.62	1.13	12.95	0.88
B-3-NF	15A	11.00	9.13	9.91†	0.53	52.47	46.94	1.12	n/a	n/a
	15B				0.54	52.86	46.32	1.14	n/a	n/a
	18A				0.53	51.97	46.42	1.12	n/a	n/a
	18B				0.59	58.22	46.67	1.25	n/a	n/a
	19A				0.49	47.51	45.20	1.05	n/a	n/a
	19B				0.45	43.39	45.07	0.96	n/a	n/a
	20A				0.43	48.22	46.10	1.05	n/a	n/a
	20B				0.58	56.48	46.62	1.21	n/a	n/a
Average		11.00	9.13	9.91	0.52	51.39	46.17	1.11	n/a	n/a

Note: See Table 1 for slab type descriptions. b_w = total web width at the centroidal axis of the slab; d_p = distance from extreme compression fiber to centroid of prestressing reinforcement; M_n = unfactored nominal moment capacity; M_{sw+app} = moment demand due to applied load and self-weight; n/a = not applicable; $V_{n,fill}$ = unfactored nominal shear capacity of core-fill concrete or grout; $V_{n,slab}$ = unfactored nominal shear capacity of slab; V_{sw+app} = shear demand due to self-weight and applied load; x_{crit} = horizontal distance from slab end to the predicted failure point. 1 in. = 25.4 mm; 1 kip = 4.448 kN.

*x_{crit} located $h/2$ from the inner face of support.

†Neglects top strands.

‡Test 12A was excluded from the averages because premature failure occurred during the test near the applied load due to nonuniform bearing at the near support.

Table 6. Comparison of EN 1168 general method predictions to experimental test results

Slab type	Test number	x_{crit}, in.	$b_w(y)$, in.	$I/S_c(y)$, in.	y, in.	V_{sw+app}, kip	V_{Rdc}, kip	V_{sw+app}/V_{Rdc}	$V_{n,fill}$, kip	V_{sw+app}/V_{Rdt}
A-1-NF	1A	11.00	19.67	9.35	4.20	86.04	74.63	1.15	n/a	n/a
	1B					73.63	74.62	0.99	n/a	n/a
	2A					79.94	74.56	1.07	n/a	n/a
	2B					77.74	74.55	1.04	n/a	n/a
Average		11.00	19.67	9.35	4.20	79.34	74.59	1.06	n/a	n/a
A-1-NF	17A	11.00	19.67	9.35	4.20	101.99	77.52	1.32	n/a	n/a
	17B					100.35	77.31	1.30	n/a	n/a
A-2-NF	16A					106.12	76.95	1.38	n/a	n/a
	16B					104.19	77.04	1.35	n/a	n/a
Average		11.00	19.67	9.35	4.20	103.16	77.21	1.34	n/a	n/a
A-1-2C	3A	11.00	19.67	9.35	4.20	73.28	71.33	1.03	22.42	0.78
	3B					88.17	71.29	1.24	22.42	0.94
	4A					72.83	74.21	0.98	22.33	0.75
	4B					89.09	74.43	1.20	22.39	0.92
Average		11.00	19.67	9.35	4.20	80.84	72.81	1.11	22.39	0.85
A-1-2R	5A	11.00	19.67	9.35	4.20	80.49	73.49	1.10	22.10	0.84
	5B					98.28	72.27	1.36	22.39	1.04
A-2-2R	6A					85.48	71.47	1.20	22.22	0.91
	6B					96.35	71.47	1.35	22.22	1.03
Average		11.00	19.67	9.35	4.20	90.15	72.17	1.25	22.24	0.96
B-3-1G	11A	12.68	9.56	9.22	5.38	54.29	40.62	1.34	21.26	0.88
	11B					53.79	40.70	1.32	21.45	0.87
	12A					41.96	43.06	0.97	22.35	0.64
	12B					49.83	42.86	1.16	22.16	0.77
	13A					48.57	42.10	1.15	22.00	0.76
	13B					52.16	42.03	1.24	22.03	0.81
	14A					55.27	42.30	1.31	21.47	0.87
	14B					50.49	42.41	1.19	21.76	0.79
Average*		12.68	9.56	9.22	5.38	52.06	41.86	1.24	21.73	0.82
B-3-NF	15A	12.68	9.56	9.22	5.38	52.42	42.36	1.24	n/a	n/a
	15B					52.82	41.90	1.26	n/a	n/a
	18A					51.93	41.55	1.25	n/a	n/a
	18B					58.09	41.73	1.39	n/a	n/a
	19A					47.47	40.73	1.17	n/a	n/a
	19B					43.35	40.62	1.07	n/a	n/a
	20A					48.17	41.29	1.17	n/a	n/a
	20B					56.44	43.73	1.29	n/a	n/a
Average		12.68	9.56	9.22	5.38	51.34	41.74	1.23	n/a	n/a

Note: See Table 1 for slab type descriptions. $b_w(y)$ = web width at height y along the line of failure; $I/S_c(y)$ = ratio of the second moment of area and the first moment of area for height y; n/a = not applicable; $V_{n,fill}$ = predicted shear capacity of core fill; V_{Rdc} = shear resistance in regions uncracked by bending for prestressed concrete hollow-core slabs; V_{Rdt} = shear resistance in regions uncracked by bending for prestressed concrete hollow-core slabs with filled cores; V_{sw+app} = shear demand due to self-weight and applied load; x_{crit} = horizontal distance from slab end to the predicted failure point; y = height of critical point on the line of failure. 1 in. = 25.4 mm; 1 kip = 4.448 kN.

*Test 12A was excluded from the averages because premature failure occurred near the applied load due to nonuniform bearing at the near support.

average failures for all tests performed on supplier A slabs occurred at shear demands that were approximately equal to or higher than the slab shear capacities predicted using EN 1168. Slabs that had lower values of concrete compressive strength at transfer (Table 2) and no core-fill concrete (tests 1A, 1B, 2A, and 2B) failed in shear at an average of 106% (±8%) of shear resistance in regions uncracked by bending for prestressed concrete hollow-core slabs V_{Rdc}. Slabs with lower values of concrete compressive strength at transfer and core-fill concrete placed in unroughened voids (tests 3A, 3B, 4A, and 4B) failed in shear at an average of 111% (±13%) of shear resistance in regions uncracked by bending for prestressed concrete hollow-core slabs V_{Rdc}. Slabs with lower values of concrete compressive strength at transfer and core-fill concrete placed in roughened voids (tests 5A, 5B, 6A, and 6B) failed in shear at an average of 125% (±13%) of shear resistance in regions uncracked by bending for prestressed concrete hollow-core slabs V_{Rdc}. Slabs with higher values of concrete compressive strength at transfer and no core-fill concrete (tests 17A, 17B, 16A, and 16B) failed in shear at an average of 134% (±4%) of shear resistance in regions uncracked by bending for prestressed concrete hollow-core slabs V_{Rdc}.

Data in Table 6 show that average failures for all tests performed on supplier B slabs (excluding slab type B-3-1E) also occurred at shear demands that were higher than the slab shear capacities predicted using EN 1168. Supplier B slabs with core-fill grout in one void (slab type B-3-1G) failed in shear at an average of 124% (±9%) of shear resistance in regions uncracked by bending for prestressed concrete hollow-core slabs V_{Rdc}, and supplier B slabs with no core-fill grout (slab type B-3-NF) failed in shear at an average of 123% (±16%) of shear resistance in regions uncracked by bending for prestressed concrete hollow-core slabs V_{Rdc}.

Discussion

Predicted values and core-fill gain assumptions

Results in Table 5 show that ACI 318-14[9] provided conservative capacity predictions for unfilled and grout-filled slabs provided by supplier B (excluding slab type B31E) with an average shear demand from self-weight and applied load V_{sw+app} to $V_{n,slab}$ ratio of 1.12, where $V_{n,slab}$ is the unfactored nominal shear capacity of extruded slab. However, an average shear demand from self-weight and applied load V_{sw+app} to capacity $V_{n,slab}$ ratio of 0.83 was found for some slabs provided by supplier A that were cast without core-fill concrete (excluding the slabs with the highest concrete compressive strength at prestressing transfer $f'_{c,transfer}$ values, which had shear demand–to–capacity ratios greater than 1.0). The shear demand from self-weight and applied load V_{sw+app} to capacity $V_{n,slab}$ ratios for some of the slabs cast with core-fill concrete (tests 3A, 4A, and 5A) were also of the same magnitude. Failures occurring below capacities predicted by ACI 318-14 for supplier A slabs could be attributed to the high moment demand that was present when failures occurred, which may not be realistic for in situ loading conditions experienced by hollow-core slab systems. A 1962 report by ACI-ASCE (American Society of Civil Engineers) Committee 326,[17] which is the basis for ACI 318-14, found that the diagonal tensile strength of concrete could vary from approximately $1.9\sqrt{f'_c}$ to $3.5\sqrt{f'_c}$ psi depending on several factors, including the longitudinal reinforcement ratio and moment demand. The ACI 318-14 web-shear capacity equation assumes the diagonal tensile strength of concrete is equal to $3.5\sqrt{f'_c}$,[17,18] based on the assumption that the moment demand M is negligible ($M \approx 0$).[17] This assumption was justifiable for supplier B slabs, where web-shear failure was the controlling failure mode due to the narrow web widths being located at or near the centroidal axis of the circular void; however, having a negligible moment demand was not the case when failures occurred in slabs provided by supplier A.

Results in Table 6 show that EN 1168[5] provided conservative predictions for slabs provided by supplier B (excluding slab type B-3-1E) with an average shear demand from self-weight and applied load V_{sw+app} to shear resistance in regions uncracked by bending for prestressed concrete hollow-core slabs V_{Rdc} ratio of 1.24. An average shear demand from self-weight and applied load V_{sw+app} to shear resistance in regions uncracked by bending for prestressed concrete hollow-core slabs V_{Rdc} ratio of 1.06 was found for slabs provided by supplier A that were cast without core-fill concrete (excluding the slabs with the highest $f'_{c,transfer}$ values, which had higher shear demand–to–capacity ratios); the shear demand from self-weight and applied load V_{sw+app} to shear resistance in regions uncracked by bending for prestressed concrete hollow-core slabs V_{Rdc} ratios for some of the slabs cast with core-fill concrete (tests 3A, 4A, and 5A) were also of the same magnitude.

For supplier B, the ratios of shear demand from self-weight and applied load V_{sw+app} to capacity $V_{n,slab}$ (Table 5) and shear demand from self-weight and applied load V_{sw+app} to shear resistance in regions uncracked by bending for prestressed concrete hollow-core slabs V_{Rdc} (Table 6) were nearly equal for slabs with and without core-fill grout for ACI 318-14 (113% with grout and 111% without grout) and EN 1168 (124% with grout and 123% without grout). This suggests that the core-fill grout did not provide additional web-shear capacity. Although the core-fill grout was added immediately after slab extrusion and prior to transfer, an evaluation of the failure planes for tests 11B, 12B (**Fig. 7**), 13B, and 14B showed that the core-fill grout material failed separately from the webs of the extruded slab and did not act compositely with the slab.

Whereas minimal additional web-shear capacity was gained from the use of core-fill grout in supplier B slabs, shear capacity gains from the addition of core-fill concrete were realized for some of the supplier A slabs. Results in Tables 5 and 6 show that the shear demand–to–capacity ratio of the slab (shear demand from self-weight and applied load V_{sw+app} to capacity $V_{n,slab}$ and shear demand from self-weight and applied load V_{sw+app} to shear resistance in regions uncracked by bending for prestressed concrete hollow-core slabs V_{Rdc}

Failure plane for test 12B showing sloped web-shear failures in the extruded slab and the vertical failure plane of core-fill grout

Test 3B failure plane showing composite action between one of two core-fill concrete sections and interior web of extruded slab

Test 4B failure plane showing continuous shear plane for one of two voids filled with concrete

Fully composite action between the core-fill concrete and interior webs for test 5B

Continuous shear plane for test 6B

Figure 7. Evaluation of failure planes from testing

for ACI 318-14 and EN 1168, respectively) for tests 3A, 4A, and 5A were nearly equal to those for tests 1A, 1B, 2A, and 2B. However, the shear demand from self-weight and applied load V_{sw+app} to capacity $V_{n,slab}$ (ACI 318-14) and shear demand from self-weight and applied load V_{sw+app} to shear resistance in regions uncracked by bending for prestressed concrete hollow-core slabs V_{Rdc} (EN 1168) ratios were greater for tests 3B, 4B, 5B, 6A, and 6B compared with tests 1A, 1B, 2A, and 2B. This suggests that additional web-shear capacity was obtained from the core-fill concrete for these tests. The failure planes for tests 3B and 4B (Fig. 7) show that core-fill concrete in one of the two filled voids acted compositely with a web of the extruded hollow-core slab. The failure planes for tests 5B and 6B (Fig. 7) show that core-fill concrete in both voids acted compositely with the webs of the extruded hollow-core slab. The walls and bottom surface of the core-filled voids were roughened in slabs 5 and 6, designated A-1-2R and A-2-2R. ACI 318-14 considers intentional surface roughening to an amplitude of 0.25 in. (6.35 mm) in section 16.4.4.2 when calculating horizontal shear strength; this amplitude of roughening, which was based on work by Hanson,[21] Kaar et al.,[22] and Saemann and Washa,[23] may promote composite action when core-filling hollow-core slabs to realize gains in web-shear capacity.

Effects of concrete compressive strength at transfer

The shear demand at failure V_{sw+app} for tests 16A, 16B, 17A, and 17B exceeded that of all other slabs provided by supplier A, including those where core-fill concrete was present in two of the five voids. The concrete compressive strength at transfer $f'_{c,transfer}$ for tests 16A, 16B, 17A, and 17B (Table 2) was approximately 2 ksi (14 MPa) greater than that of any other slab tested. The higher value for $f'_{c,transfer}$ likely resulted in an improved bond between the prestressing strands and hollow-core slab, which reduced the transfer (transmission) length for the prestressing strands and resulted in the prestressing force being transferred to the extruded slab more effectively. The reduction in transfer length resulted in failures for slabs 16 and 17 occurring closer to the support (where the moment demand was lower), but failure in typical slabs from supplier A occurred closer to the point of applied load (**Fig. 8**).

According to EN 1168,[5] a reduction in the transmission length will result in a higher loss of shear capacity due to shear stresses within the transmission length region (that is, more concrete shear stress $\tau_{cp}(y)$ to subtract). However, a shorter transmission length can also remove shear stresses from the region near the maximum moment demand (point of applied load in this test setup), where the combination of shear stress and moment demand can generate a larger loss in web-shear capacity. For slab 17A, given the 6640 psi (45.8 MPa) concrete compressive strength at transfer and the low 0.03 in. (0.8 mm) initial strand slip that was recorded prior to testing, calculations were performed assuming a shorter transmission length of l_{pt} of 14.6 in. (370 mm) based on EN 1168 failure location assumptions. **Figure 9**

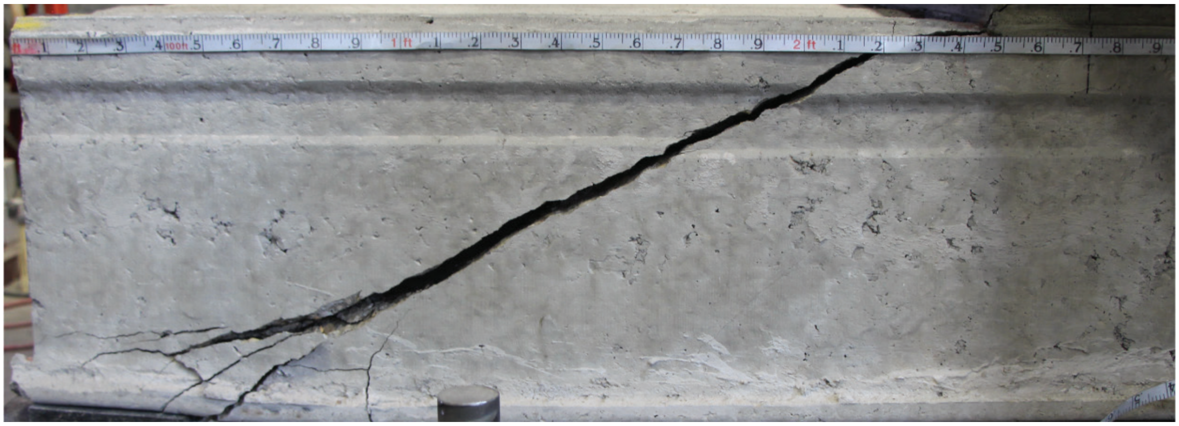

Test 17A web-shear crack at failure closer to support

Test 1A web-shear crack at failure closer to point of applied load

Figure 8. Differences in web-shear failure location due to the concrete compressive strength at transfer.

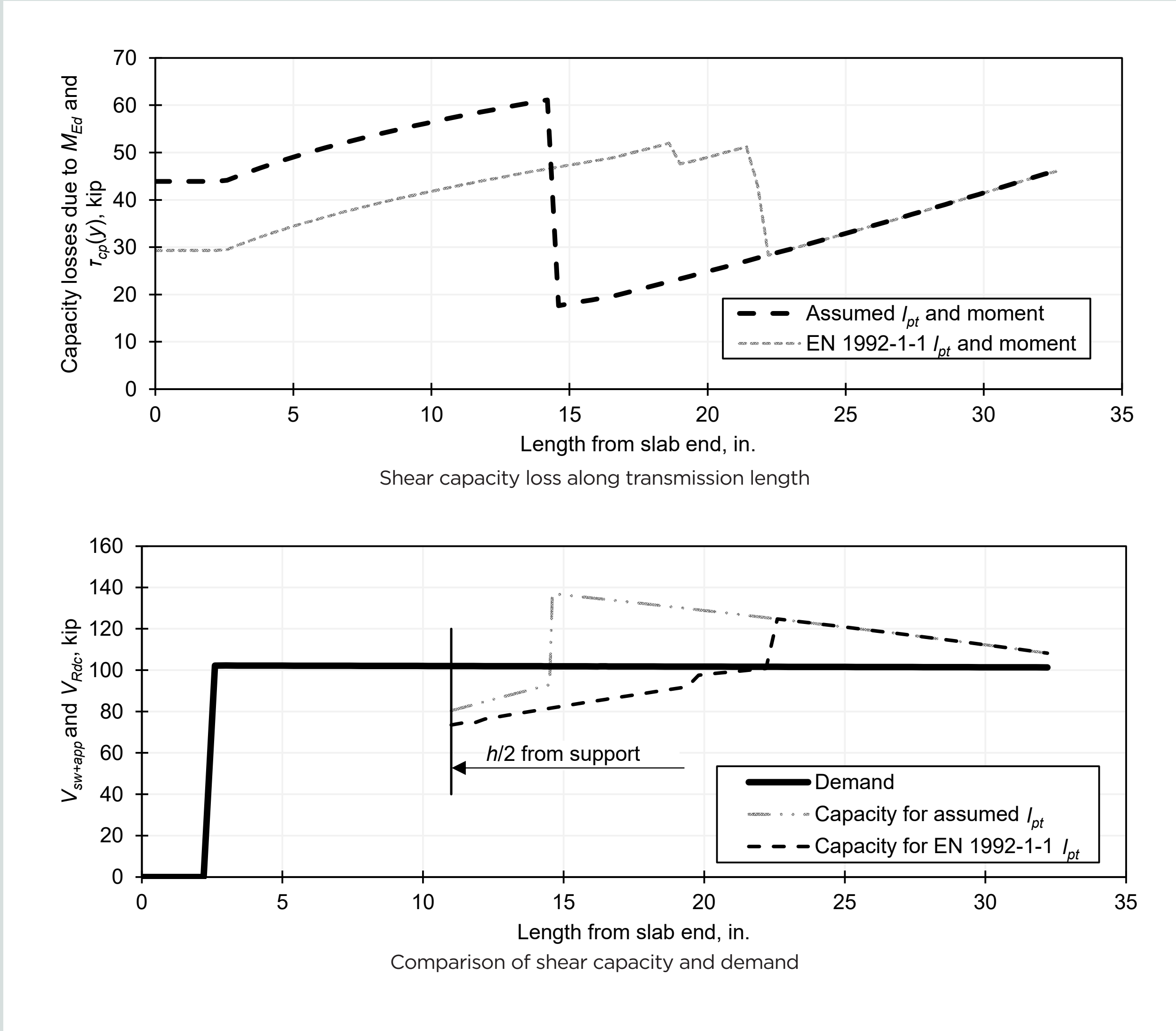

Figure 9. Shear capacity loss along transmission length and comparison of shear capacity and demand for slab 17A.
Note: Shear capacity loss is the sum of the EN 1168 losses due to applied moment from the actual load at failure and shear stresses within the transmission length. The comparison of shear capacity and demand shows the demand at failure V_{sw+app} and both the EN 1168–predicted capacity V_{Rdc} for the assumed l_{pt} and the EN 1168–predicted capacity V_{Rdc} for the EN 1992-1-1–predicted l_{pt}. h = height of hollow-core slab; l_{pt} = prestressing strand transmission length; M_{Ed} = bending moment due to the vertical load; V_{Rdc} = shear resistance in regions uncracked by bending for prestressed concrete hollow-core slabs; V_{sw+app} = shear demand due to self-weight of extruded slab and applied load; $\tau_{cp}(y)$ = concrete shear stress due to transmission of prestress at height y and distance l_x. 1 in. = 25.4 mm; 1 kip = 4.448 kN.

shows the sum of the EN 1168 losses in shear capacity due to applied moment from the actual load at failure (117.9 kip [524.4 kN]) and due to shear stresses within the transmission length (for both the l_{pt} of 22.3 in. [566 mm] predicted by EN 1992-1-1[19] and the assumed l_{pt} of 14.6 in.) for slab 17A. The data series show that there may be up to 50 to 60 kip (220 to 270 kN) of shear capacity lost within the transmission length; however, shear capacity losses are only due to the applied moment after the transmission length. Figure 9 shows the shear demand and the corresponding EN 1168 capacity predictions for slab 17A due to the actual applied load at failure. There is relatively little difference in the capacity predictions if failures had occurred near the member height from the face of the support, but differences in capacity become more pronounced and dependent on the transfer length as the location of interest moves toward the point of applied load.

The increase in web-shear capacity closer to the support (assuming a shorter transmission length) would also explain the very consistent failure loads for tests 16A and 16B (failures at 121 ± 1 kip [538 ± 4 kN]) and for tests 17A and 17B (failures at 117 ± 1 kip [520 ± 4 kN]). In these cases, the failure mode was more predictable because it likely occurred outside of the transmission length where shear stresses act but away from the location with the highest moment demand.

Effects of total prestressing force

Truderung and associates[14] noted that ACI 318-14[9] predicted increased web-shear capacities as the total prestressing force increased, but the predictions were not upheld when they tested slabs that were almost identical to those provided by supplier B in this research program. Truderung and associates found that slabs with prestressing strands tensioned with a jacking stress at the neutral axis of 1.00 ksi (6.90 MPa) failed at 146% of the predicted shear capacity, and slabs cast with a jacking stress at the neutral axis of 1.48 ksi (10.20 MPa) failed at 90% of the predicted shear capacity. In this research program, supplier B slabs with prestressing strands tensioned with a jacking stress at the neutral axis of 1.20 ksi (8.27 MPa) failed at 112% of the shear capacity predicted by ACI 318-14. The shear demand–to–capacity ratio for supplier B slabs at failure corresponded well with the findings of Truderung et al. Those investigators also found that shear capacity predictions using EN 1168 were more accurate for the slabs tested as part of their program and noted that the traditional North American approach to hollow-core design fails to incorporate variables that affect capacity, such as the cross-sectional geometry and the shear stresses that are induced by the prestressing strands (such as those calculated with Eq. [7]). These findings suggest two concepts: there may exist an optimal jacking stress at the neutral axis that maximizes the shear capacity of a hollow-core slab (that is, that a hollow-core slab can be overstressed, resulting in reduced shear capacity), and ACI 318-14 may not incorporate one or more important variables when predicting web-shear capacity of hollow-core slabs (for example, moment demand or shear stresses from the prestressing strands, or both).

The first concept is supported by test results for slabs provided by supplier A. Tests 16A and 16B were performed on a slab fabricated with strand pattern type 2, which had a jacking stress at the neutral axis of 0.99 ksi (6.83 MPa), and tests 17A and 17B were performed on a slab fabricated with strand pattern type 1, which had a jacking stress at the neutral axis of 1.13 ksi (7.79 MPa). The shear demand at failure for tests 16A and 16B slightly exceeded those for tests 17A and 17B. Average failures occurred at 112.5% of capacity predicted by ACI 318-14 during tests 16A and 16B, compared with 108.5% during tests 17A and 17B. Average failures occurred at 136.5% of capacity predicted by EN 1168[5] during tests 16A and 16B, compared with 131% during tests 17A and 17B. These average failure results were achieved even though the concrete compressive strengths when the slabs were tested were approximately equal and concrete compressive strengths at transfer were higher for slab tests 17A and 17B.

Truderung and associates[14] also found that the actual failure location shifted away from the support and toward the load application point as the jacking stress at the neutral axis was increased, which was the case for most slabs tested as part of this program. The general method of EN 1168 explains this phenomenon. As the jacking stress at the neutral axis is increased, the transmission length, the magnitude of the shear stresses, or a combination of the two will also increase. Higher jacking stresses at the neutral axis may result in greater reduction of web-shear capacity near the point of applied load due to combined shear stresses and moment demand, and that reduced capacity may result in failures that occur farther away from the support; this was observed for most tests on supplier A slabs in this program.

Conclusion

The following conclusions were formed based on the results of this research program:

- Composite action between the core-fill material (concrete or grout) and the hollow-core slab is necessary where core-fill material is expected to increase the web-shear capacity.

- Design methodologies should account for shear stresses within the transmission (transfer) length when predicting the shear capacity of hollow-core slabs. The magnitude of the shear stress will increase if the transmission (transfer) length is held constant and the jacking stress is increased. This may result in failures occurring farther from the support (closer to the load application point) if the critical location for failure is within the transmission (transfer) length.

- An optimal jacking stress may exist that maximizes the web-shear capacity of extruded hollow-core slabs. The general method of EN 1168[5] suggests that, depending on the moment demand and the transmission (transfer) length of the prestressing strands, an increase in jacking stress may result in a loss of shear capacity at a failure location near the load point. Increasing the amount of prestressing force may not necessarily result in increased web-shear capacity.

- Moment demand from applied load and self-weight affects the web-shear capacity of hollow-core slabs with noncircular voids loaded similarly to those in this research program. Web-shear capacity will potentially increase with reduced moment demand. Slabs with noncircular voids and thick webs had both high shear and high moment demands at failure relative to the respective capacity. These slabs failed at shear demand–to–capacity ratios that were lower than slabs with circular voids, narrow webs, and moment demands that were approximately half of the predicted capacity.

- Increasing the concrete compressive strength at transfer and therefore reducing the transfer length may result in higher web-shear capacity gains compared with those expected from filling cores with concrete or grout. Although this relationship between transfer length and shear capacity has always been assumed in conventional shear design (ACI 318-14[9] and EN 1992-1-1[19]), it becomes more apparent for hollow-core slabs with noncircular voids that are subject to high moment demands when considering shear stresses as proposed by EN 1168.

Recommendations

The following recommendations are based on the results of this research program:

- Future research on the shear capacity of hollow-core slabs should include uniform loading during testing to eliminate the potential for premature failures occurring due to unintended torsional stresses or stress concentrations. This objective might be accomplished by using a rotating (self-adjusting) support system, like that described by Pajari.[7]

- Minimum requirements to promote composite action and form a bond between the core-fill material and the extruded slab should be established if shear capacity gains from the use of core-fill concrete or grout are assumed. These could include roughening void walls and immediately adding fill material following slab extrusion.

- Novel core-filling techniques, such as those investigated by McDermott and Dymond,[12] should be reevaluated with fill material that is placed in voids where the walls have been roughened to promote composite action.

- Research should be performed to investigate the ideal roughening amplitude required to achieve bond between a hollow-core slab and concrete or grout-based core-fill material.

- The optimal cross-sectional location of core-fill concrete or grout should be investigated. Shear capacity in hollow-core slabs is often governed by the weakest web, which is usually an exterior web where only a single prestressing strand may be used. If possible, placement of core-fill concrete or grout in voids next to exterior webs may provide greater capacity gains than can be achieved with core fill placed in interior voids.

- The effect that moment demand and capacity may have on the web-shear capacity of hollow-core slabs should be investigated further. Additional research should determine whether increasing the moment capacity relative to moment demand at failure might increase the web-shear capacity of prestressed concrete hollow-core slabs as implied by the ACI-ASCE Committee 316 report.[17] The research should also consider that, at some point, increased prestressing force may no longer provide additional web-shear capacity and, in fact, may result in a reduction of web-shear capacity due to shear stresses that are induced.

- Systems of hollow-core slabs (that is, multiple hollow-core slabs placed side by side with grouted shear keys) should be tested to evaluate how load distribution within the system may affect the shear capacity of one or more hollow-core slabs. Testing an individual slab may not accurately reflect the shear capacity of a hollow-core slab floor system where there is a likelihood that load and loading eccentricities are distributed within the system.

Acknowledgments

The authors are sincerely grateful for the generous donations of time and material from the hollow-core suppliers, without which this research would not have been possible. Assistance from many students in the structures laboratory at the University of Minnesota Duluth was also invaluable.

References

1. PCI Hollow Core Slab Producers Committee. 2015. *PCI Manual for the Design of Hollow Core Slabs and Walls*. MNL-126. 3rd ed. Chicago, IL: PCI.

2. Anderson, A. R. 1978. *Shear Strength of Hollow Core Members*. Technical bulletin 78-B1. Tacoma, WA: Concrete Technology Associates.

3. Anderson, R. G. 1987. *Web Shear Strength of Prestressed Concrete Members*. Technical bulletin 85B1. Tacoma, WA: Concrete Technology Associates.

4. SMA (Spancrete Manufacturers Association). 2010. *Shear Strength with Filled Cores*. Research note 1007. Waukesha, WI: SMA.

5. CEN (European Committee for Standardization). 2011. *Precast Concrete Products—Hollow Core Slabs*. EN 1168:2005+A3:2011. Brussels, Belgium: CEN.

6. Yang, L. 1994. "Design of Prestressed Hollow-core Slabs with Reference to Web Shear Failure." *Journal of Structural Engineering* 120 (9): 2675–2696. https://doi.org/10.1061/(ASCE)0733-9445(1994)120:9(2675).

7. Pajari, M. 2005. *Resistance of Prestressed Hollow Core Slabs against Web Shear Failure*. VTT Technical Research Centre of Finland research notes 2292. https://www.vttresearch.com/sites/default/files/pdf/tiedotteet/2005/T2292.pdf.

8. Pajari, M. 2009. "Web Shear Failure in Prestressed Hollow Core Slabs." *Rakenteiden Mekaniikka* [Journal of Structural Mechanics] 42 (4): 207–217.

9. ACI (American Concrete Institute) Committee 318. 2014. *Building Code Requirements for Structural Concrete (ACI 318-14) and Commentary (ACI 318R-14)*. Farmington Hills, MI: ACI.

10. Hawkins, N. M, and S. K. Ghosh. 2006. "Shear Strength of Hollow-Core Slabs." *PCI Journal* 51 (1): 110–114.

11. Palmer, K. D., and A. E. Schultz. 2011. "Experimental Investigation of the Web-Shear Strength of Deep Hollow-Core Units." *PCI Journal* 56 (4): 83-104. https://doi.org/10.15554/pcij.09012011.83.104.

12. McDermott, M. R., and B. Z. Dymond. 2020. "Shear Capacity of Hollow-Core Slabs with Concrete-Filled Cores." *PCI Journal* 65 (2): 59–74. https://doi.org/10.15554/pcij65.2-03.

13. Lee, D., M. Park, H. Joo, S. Han, and K. S. Kim. 2020. "Strengths of Thick Prestressed Precast Hollow Core Slab Members Strengthened in Shear." *ACI Structural Journal* 117 (2): 129–140. doi: 10.14359/51720203.

14. Truderung, K. A., A. El-Ragaby, M. Mady, and E, El-Salakawy. 2019. "Shear Capacity of Dry-Cast Extruded Precast, Prestressed Concrete Hollow-Core Slabs." *PCI Journal* 64 (4): 71-83. https://doi.org/10.15554/pcij64.4-01.

15. ASTM International. 2017. *Standard Test Method for Compressive Strength of Cylindrical Concrete Specimens*. ASTM C39/C39M-17b. West Conshohocken, PA: ASTM International.

16. ACI and ASCE (American Society of Civil Engineering) Joint Committee 423. 2016. *Guide to Estimating Prestress Loss.* ACI 423.10R-16. Farmington Hills, MI: ACI.

17. ACI-ASCE Committee 326. 1962. "Shear and Diagonal Tension." *ACI Journal* 59 (2): 277-333. https://doi.org/10.14359/7920.

18. Macgregor, J. G., and J. M. Hanson. 1969. "Proposed Changes in Shear Provisions for Reinforced and Prestressed Concrete Beams." *ACI Journal* 66 (4): 276-288. https://doi.org/10.14359/7360.

19. CEN. 2004. *Eurocode 2: Design of Concrete Structures—Part 1-1: General Rules and Rules for Buildings*. EN 1992-1-1. Brussels, Belgium: CEN.

20. Asperheim, S. A. 2020. "Variation in Web-shear Capacity of Hollow-Core Slabs with Filled Cores." MS thesis, University of Minnesota Duluth.

21. Hanson, N. W. 1960. "Precast-Prestressed Concrete Bridges: Horizontal Shear Connections" *Journal of the PCA Research and Development Laboratories* 2 (2): 38–58.

22. Kaar, P. H., L. B. Kriz, and E. Hognestad. 1960. "Precast-Prestressed Concrete Bridges: (1) Pilot Tests of Continuous Girders." *Journal of the PCA Research and Development Laboratories* 2 (2): 21–37.

23. Saemann, J. C., and G. W. Washa. 1964. "Horizontal Shear Connections between Precast Beams and Cast-in-Place Slabs." *Journal of the American Concrete Institute* 61 (11): 1383–1409.https://doi.org/10.14359/7832.

Notation

a = shear span

A = fictive cross-section surface

A_c = cross-sectional area of hollow-core slab

$A_c(y)$ = area above height y

A_f = cross-sectional area of filled core

b_c = width of the cores

b_w = width of web(s)

$b_w(y)$ = web width at the height y

$C_{pt}(y)$ = factor taking into account the position of the considered tendon layer

d = distance from extreme compression fiber to centroid of longitudinal tension reinforcement

d_b = nominal strand diameter of the prestressing strand

d_p = distance from extreme compression fiber to centroid of prestressing reinforcement

$\frac{dP_t(l_x)}{dx}$ = gradient of the prestressing force in the considered tendon layer at a distance l_x

f'_c = nominal compressive strength of hollow-core slab concrete when tested

f'_{cf} = average compressive strength of core-fill material on slab test day

f_{ct} = actual tensile strength of concrete

$f_{ct,f}$ = actual tensile strength of core-fill material

f_{ctd} = design tensile strength of concrete

$f_{ctd,f}$ = design tensile strength of core-fill material

$f'_{c,transfer}$ = concrete compressive strength at prestressing transfer

f_{pc} = compressive stress in concrete, after allowance for all prestress losses, at centroid of cross section resisting externally applied loads

f_{pu} = ultimate tensile strength of prestressing strands

f'_t = diagonal tension strength of concrete defined by the American Concrete Institute

F_j = prestressing strand jacking force

h = height of hollow-core slab

I = second moment of area of the cross section

l_{pt} = prestressing strand transmission length

l_{tr} = prestressing strand transfer length

l_x = distance of section considered from the starting point of the transmission length

L = length of hollow-core section

M = moment demand

M_{Ed} = bending moment due to the vertical load

M_n = unfactored nominal moment capacity of extruded slab

M_{sw+app} = moment demand due to self-weight of extruded slab and applied load

n_f = number of filled cores

$P_t(l_x)$ = prestressing force in the considered tendon layer at a distance l_x

$S_c(y)$ = first moment of the area above height y and about the centroidal axis

V_c = nominal shear strength provided by concrete

V_{cw} = nominal shear capacity provided by concrete where diagonal cracking results from high principal tensile stress in web

$V_{n,fill}$ = unfactored nominal shear capacity of core-fill concrete or grout

$V_{n,slab}$ = unfactored nominal shear capacity of extruded slab

V_p = vertical component of effective prestressing force at section

V_{Rdc} = shear resistance in regions uncracked by bending for prestressed concrete hollow-core slabs

V_{Rdt} = shear resistance in regions uncracked by bending for prestressed concrete hollow-core slabs with filled cores

V_{sw+app} = shear demand due to self-weight of extruded slab and applied load

x_{crit} = horizontal distance from the slab end to the predicted failure location

y = height of critical point on the line of failure

Y_c = height of the centroidal axis

Y_{Pt} = height of the position of considered tendon layer

$\sigma_{cp}(y)$ = full concrete compressive stress at height y and distance l_x

$\tau_{cp}(y)$ = concrete shear stress due to transmission of prestress at height y and distance l_x

About the authors

Scott Asperheim is a technical sergeant in the U.S. Air Force. He received his BS and MS in civil engineering from the University of Minnesota Duluth, having focused on structural engineering.

Benjamin Dymond, PhD, is an associate professor in the Civil Engineering Department and the director of the Resilient Precast Concrete Certificate Program at the University of Minnesota Duluth. His research interests include design and analysis of concrete structural systems and their components, experimental investigations, and long-term structural monitoring.

Abstract

Since the 1970s, hollow-core slab manufacturers have filled voids with concrete to increase shear capacity, but limited research into the efficacy of this practice has been completed. Forty tests were performed on 20 hollow-core slabs that were 12 in. (300 mm) deep to quantify the variation in web-shear capacity that can be gained. The 20 slabs had either no core fill, cores filled with concrete or grout, or one void omitted during fabrication. Two different cross sections were investigated, a heavy-duty slab with thick webs and noncircular voids and a slab with narrow webs and circular voids. The results indicated that adequate composite action between the core-fill material and extruded slab was necessary to realize web-shear capacity gains. In addition, the prestressing strand jacking stress, concrete compressive strength at transfer, transfer length, and moment demand can have a large effect on the web-shear capacity of a hollow-core slab.

Keywords

ACI 318, bond, core fill, EN 1168, hollow-core slab, moment demand, roughened surface, shear capacity, shear stress, web shear.

Review policy

This paper was reviewed in accordance with the Precast/Prestressed Concrete Institute's peer-review process.

Reader comments

Please address any reader comments to *PCI Journal* editor-in-chief Tom Klemens at tklemens@pci.org or Precast/Prestressed Concrete Institute, c/o *PCI Journal*, 8770 W. Bryn Mawr Ave., Suite 1150, Chicago, IL 60631.